



ORIGINAL ARTICLE

1st Nano Update

Biosynthesis of Au nanoparticles using olive leaf extract

Mostafa M.H. Khalil *, Eman H. Ismail, Fatma El-Magdoub

Chemistry Department, Faculty of Science, Ain Shams University, Abbassia, Cairo, Egypt

Received 20 October 2010; accepted 25 November 2010

Available online 28 November 2010

KEYWORDS

Biosynthesis;
Gold nanoparticles;
Olive leaf extract;
Antioxidant

Abstract The biological synthesis of gold nanoparticles (AuNPs) of various shapes (triangle, hexagonal, and spherical) using hot water olive leaf extracts as reducing agent is reported. The size and the shape of Au nanoparticles are modulated by varying the ratio of metal salt and extract in the reaction medium. Only 20 min were required for the conversion into gold nanoparticles at room temperature, suggesting a reaction rate higher or comparable to those of nanoparticles synthesis by chemical methods. The variation of the pH of the reaction medium gives AuNPs nanoparticles of different shapes. The nanoparticles obtained are characterized by UV–Vis spectroscopy, photoluminescence, transmission electron microscopy (TEM), X-ray diffraction (XRD), FTIR spectroscopy and thermogravimetric analysis. The TEM images showed that a mixture of shapes (triangular, hexagonal and spherical) structures was formed at lower leaf broth concentration and high pH, while smaller spherical shapes were obtained at higher leaf broth concentration and low pH.

© 2010 King Saud University. Production and hosting by Elsevier B.V. All rights reserved.

1. Introduction

Gold nanoparticles have been considered as an important area of research due to their unique and tunable surface plasmon

resonance (SPR) and their applications in biomedical science including drug delivery, tissue/tumor imaging, photothermal therapy and immuno-chromatographic identification of pathogens in clinical specimens (Huang, 2006). Due to the recent increasing awareness of green chemistry, it must be a nontoxic and environmentally friendly chemical. The integration of green chemistry principles to nanotechnology is one of the key issues in nanoscience research. Since the development of the concept of green nanoparticle preparation by Raveendran et al. (2003), there is a growing the need for environmentally benign metal–nanoparticle synthesis processes that do not use toxic chemicals in the synthesis protocols to avoid adverse effects in medical applications. Both Ag and Au nanoparticles are excellent nanomaterials providing a powerful platform in biomedical applications of biomolecular recognition, biosen-

* Corresponding author. Tel.: +20 145787758.
E-mail address: khalil62@yahoo.com (M.M.H. Khalil).

1878-5352 © 2010 King Saud University. Production and hosting by Elsevier B.V. All rights reserved.

Peer review under responsibility of King Saud University.
doi:10.1016/j.arabjc.2010.11.011



Production and hosting by Elsevier

sing, drug delivery and molecular imaging (Sperling et al., 2008; Wilson, 2008).

Many biological systems, such as that of fungi (Raveendran et al., 2003; Shankar et al., 2003), algae (Xie et al., 2007; Mata et al., 2009), bacteria (Lengke et al., 2006; He et al., 2008) and plants (Philip, 2009, 2010; Rajasekharreddy et al., 2010; Dubeya et al., 2010; Smitha et al., 2009; Song et al., 2009; Thakkar et al., 2010; Shankar et al., 2004; Ankamwar et al., 2005; Ghodake et al., 2010; Kalishwaralal et al., 2010; Kumar and Yadav, 2008; Chandran et al., 2006; Mishra et al., 2010; Das et al., 2010; Krpeti et al., 2009) have been studied for the biosynthesis of gold and silver nanoparticles. However, plant-based nanoparticle syntheses can be advantageous over other biological methods (microbial) since the reaction rate for the synthesis of nanoparticles is very high and there is no need to grow microbes (Kalishwaralal et al., 2010).

Throughout the history of civilization, the olive plant has been an important source of nutrition and medicine. The first formal report of medicinal use was made in 1854, when olive leaf extract (OLE) was reported to be effective in treating fever and malaria (Hanbury, 1854). OLE contains compounds with potent antimicrobial activities against bacteria, fungi, and mycoplasma (Juven and Henis, 1970; Aziz et al., 1998; Bisignano et al., 1999; Furneri et al., 2002). In addition, OLE has antioxidant (Ziogas et al., 2010; Caruso et al., 1999; Lee et al., 2009; Benavente-García et al., 2000) and anti-inflammatory (Visioli et al., 1998; de la Puerta et al., 2000) activities. Also, it was found that OLE inhibits acute infection and cell-to-cell transmission of HIV-1 and also inhibits HIV-1 replication (Lee-Huang et al., 2003).

The major active components in olive leaf are known to be oleuropein and its derivatives, such as hydroxytyrosol and tyrosol, as well as caffeic acid, p-coumaric acid, vanillic acid, vanillin, luteolin, diosmetin, rutin, luteolin-7-glucoside, apigenin-7-glucoside, and diosmetin-7-glucoside (Bianco and Uccella, 2000; Farag et al., 2003).

So far, there is no report on the synthesis of nanoparticles using olive leaf extracts. In this paper we report on the synthesis of gold nanoparticles using hot water olive leaf extracts as a simple, low cost and reproducible method.

2. Experimental

2.1. Materials

$\text{HAuCl}_4 \cdot 3\text{H}_2\text{O}$ 99.9% was purchased from Aldrich. The 1.0 g of olive leaf broth was boiled for 15 min, filtrated and completed to 100 ml to get the extract. The filtrate that was used as reducing agent was kept in the dark at 10 °C to be used within 1 week. A stock solution of HAuCl_4 was prepared by dissolving 1.0 g HAuCl_4 in 100 ml deionized water.

2.2. Instrumentation

The UV–Vis spectra were recorded at room temperature using a λ -Helios SP Pye-Unicam spectrophotometer with samples in quartz cuvettes. Photoluminescence spectra were recorded on a Perkin–Elmer LS 50B luminescence spectrophotometer.

Transmission electron microscopy (TEM) studies were performed using a JEOL-JEM 1200 electron microscope operating at an accelerating voltage of 90 kV. For the TEM mea-

surements, a drop of solution containing the particles was deposited on a copper grid covered with amorphous carbon. After allowing the film to stand for 2 min, the extra solution was removed by means of blotting paper and the grid allowed drying before the measurement. Fourier transform infrared (FTIR) spectra were recorded at room temperature on a Nicolet 6700 FTIR spectrometer. For the FTIR measurements of capped gold nanoparticles, a small amount of gold nanoparticles (0.01 g) dried at 60 °C for 4 h were mixed with KBr to form a round disk suitable for FTIR measurements. To obtain the FTIR spectrum of the extract, an appropriate amount of the extract was mixed with KBr. Thermogravimetric analyses were carried out with a heating rate of 10 °C/min using a Shimadzu DT-50 thermal analyzer.

2.3. Synthesis of gold nanoparticles

For the synthesis of the gold nanoparticles, a certain volume of the olive leaf extract (0.1–6 ml) was added to the $\text{HAuCl}_4 \cdot 3\text{H}_2\text{O}$ solution and the volume was adjusted to 10 ml with de-ionized water. The final concentration of Au was 1.3×10^{-4} M. The reduction process of Au^{3+} to Au nanoparticles was followed by the change in the color of the solution from yellow to violet to dark pink and green depending on the extract concentration.

The nanoparticles prepared at different pH values, the pH of the solutions (1.3×10^{-4} M AuCl_4^- and 2 ml extract in 10 ml flask) were adjusted using 0.1 N HCl or 0.1 N NaOH solutions.

3. Results and discussion

3.1. UV–Vis spectra of gold nanoparticles

The formation and stability of gold nanoparticles were followed by UV–Vis spectrophotometry. Fig. 1 shows the UV–Vis spectra of gold nanoparticles formation using a constant HAuCl_4 concentration (1.3×10^{-4} M) with different concentrations of the extract. The inset shows photos of the color change of the gold nanoparticles with a changing olive leaf extract concentration. The violet, pink to dark pink color observed is characteristic for the surface plasmon reso-

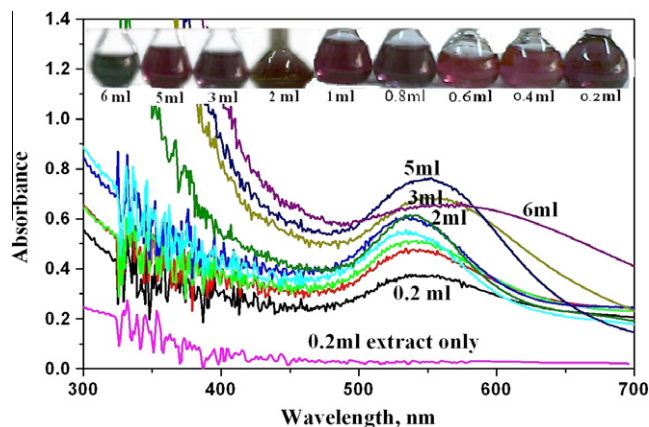


Figure 1 Effect of extract concentration on the formation of gold nanoparticles. Inset photos of the particle solutions as a function of concentration of olive leaf extract.

nance (SPR) of different sizes of gold nanoparticles (Link and El Sayed, 2000). The leaf broth extract quantities were varied from 0.2 to 6 ml. Notably, in the range of low amounts of the leaf extract (0.2–2 ml in 10 ml metal ion solution), the absorption spectra exhibit a gradual increase of the absorbance accompanied with a shift in the λ_{max} from 545 to 530 nm. On the other hand, upon addition of higher amounts of the extract (3–6 ml), the λ_{max} was shifted to longer wavelengths and the green color of the AuNPs solution was developed (inset of Fig. 1). Above 5 ml there is a slight decrease in the absorption and a negligible change in the absorbance indicating the attainment of the saturation in the bio-reduction of Au^{3+} . The absorption maximum at about 545 nm attributed to the surface plasmon resonance band of the gold nanoparticles. The interaction of light having wavelength smaller than the particle size of the AuNPs leads to a polarization of free conduction electrons with respect to the heavier ionic core of the AuNPs. Therefore, an electron dipolar oscillation is created and a surface plasmon absorption band is obtained.

A strong correlation between the particle size and the maximum absorption peak has been previously observed by Husseiny et al. (2007). They observed that as the particle size increases, the maximum absorption is red shifted. Accordingly, it can be concluded that the size of the particles decreases upon increasing the extract concentration from 0.2 to 2 ml as the absorption spectra are blue shifted (Hostetler et al., 1998). The slight red shift in λ_{max} accompanied with a slight increase in the absorbance values at longer wavelengths (600 nm) with an increase in the extract concentration from 3 to 6 ml is consistent with previously reported results for surfactant- (Aslan and Perez-Luna, 2002) and DNA-coated (Xu and Craig, 2005) gold nanoparticles and are most likely due to changes in the dielectric properties of the layer immediately surrounding the gold nanoparticles (Mulvaney, 1996; Schmidt et al., 1999) and to some small amount of particle aggregation.

Fig. 2 shows the UV–Vis spectra of the AuCl_4^- solution after the addition of 1 ml extract as a function of time. The spectra comprise a fast increasing absorption peak at about 535 nm within the first 20 min (inset of Fig. 2) followed by very slow increase in absorption. An additional absorption band at ca. 660 nm was developed after 30 min from the beginning of

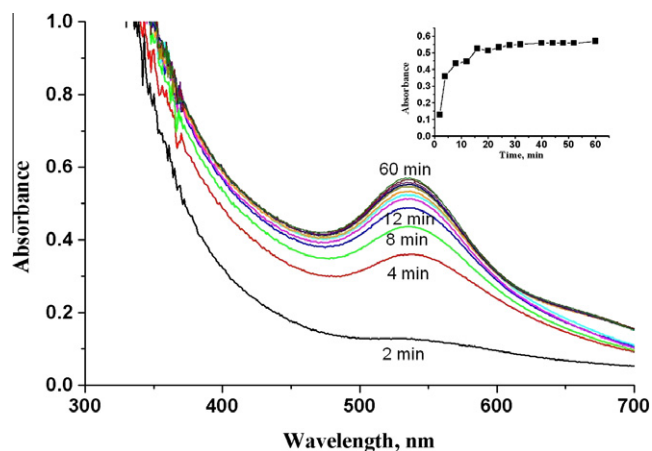


Figure 2 Kinetics of the formation of AuNPs. $\text{AuCl}_4^- = 1.3 \times 10^{-4}$ M, 1 ml extract in 10 ml flask.

the reaction. The peak at 535 nm is characteristic for the transverse plasmon resonance of AuNPs, whereas the peak at 660 nm is characteristic for the longitudinal plasmon resonance of either Au nanorods or triangular or hexagonal shaped AuNPs (Shankar et al., 2003; Daniel and Astruc, 2004). It can be concluded that the reduction of Au^{3+} using olive leaf extract occurs within 30 min.

3.2. Photoluminescence of AuNPs

Nano-metals like Au and Ag are reported (Philip, 2009; Smitha et al., 2008) to exhibit a visible photoluminescence. The fluorescence spectra of the nanoparticles formed as a function of OLE concentration are shown in Fig. 3. All the Au nanoparticles formed were found to be luminescent with an emission at 425 nm for an excitation at 350 nm. The leaf broth itself is found to be luminescent with an emission at 435 nm when it is excited with 350 nm and this luminescence of the leaf broth plays an important role for the luminescent properties of Au nanoparticles. It can be seen that increasing the extract concentration increases the fluorescence intensity reaching a maximum after the addition of 2 ml of the extract. This is consistent with the increase in the absorption spectra in Fig. 1. On the other hand, a further increase of the extract concentration leads to fluorescence quenching. This luminescence at 425 nm may be due to the functionalization of the Au nanoparticles with proteins or antioxidants present in the extract. Similar PL spectra with a band around 522 nm were reported in biotin functionalized gold nanoparticles (Kato and Caruso, 2005; Haick, 2007). Gold nanoparticles synthesized using *Pseudomonas aeruginosa* are also reported (Husseiny et al., 2007) to be photoluminescent with emission bands in the range from 565 to 595 nm.

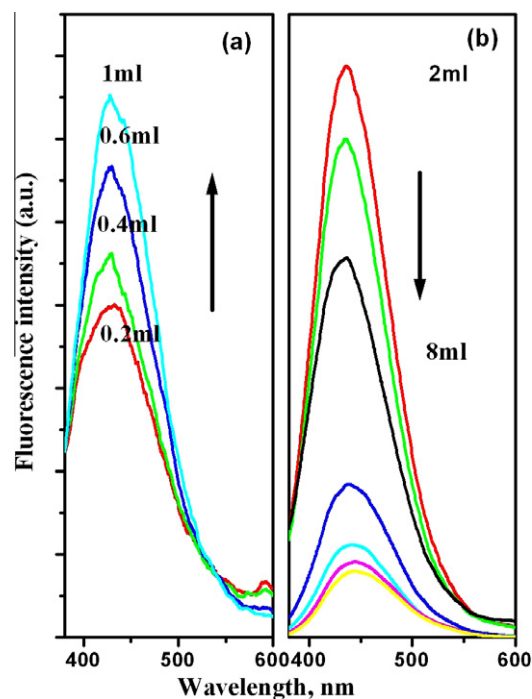


Figure 3 Fluorescence spectra of AuNPs formed as a function of extract concentration.

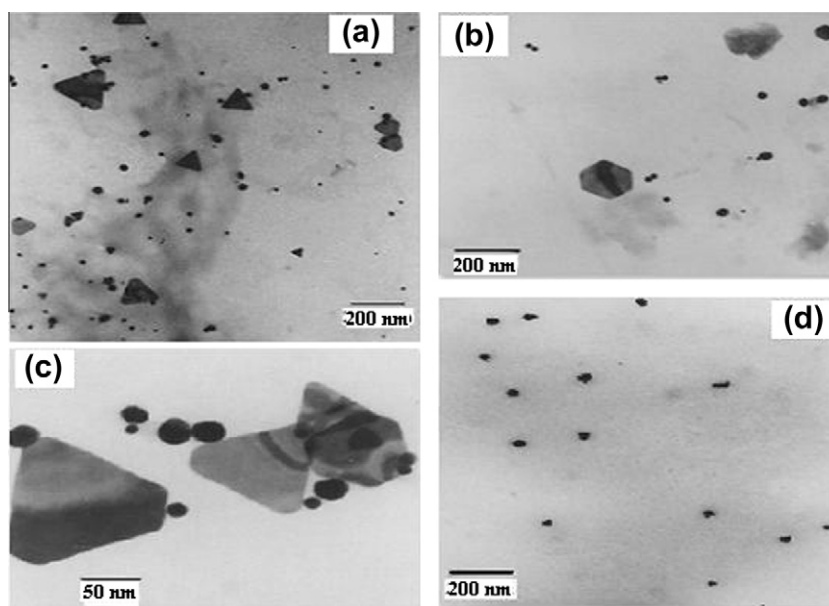


Figure 4 Effect of the leaves extract quantity on the size and shape of the AuNPs. (a) TEM image measured at 0.5 ml extract shows triangle shapes; (b) TEM image measure at 0.5 ml shows hexagonal shapes; (c) close view of triangle shape of (a); (d) shape of AuNPs formed at 5 ml of extract.

3.3. TEM and FTIR of gold nanoparticles

In Fig. 4, the TEM images clearly indicate the size and shape of the nanoparticles as a function of extract concentration. Utilizing olive leaf extracts as reducing agents at low extract concentrations (0.5 ml) the formed gold nanoparticles were predominantly nanotriangle in shape, with diameters ranging from 50 to 100 nm. Some gold nanohexagons were also present (Fig. 4a–c), as clearly shown in the TEM images. When higher

extract concentrations are used (5 ml), the nano triangular and hexagon structures disappear and the predominant nearly spherical gold nanoparticles are formed (Fig. 4d). This shows that using an excess of the extract to reduce the aqueous HAuCl_4 , the biomolecules acting as capping agents supporting the formation of shaped spherical nanoparticles rather than the formation of nano triangular or hexagonal structures. Low quantities of the extract can reduce the chloroaurate ions, but do not protect most of the quasi-spherical nanoparticles from aggregating because of the deficiency of biomolecules to act as protecting agents. Similar studies showed that the comparatively higher extract ratio is responsible for the synthesis of symmetrical nanoparticles (Sosa et al., 2003).

FTIR measurements were carried out to identify the potential biomolecules in olive leaf responsible for the reduction,

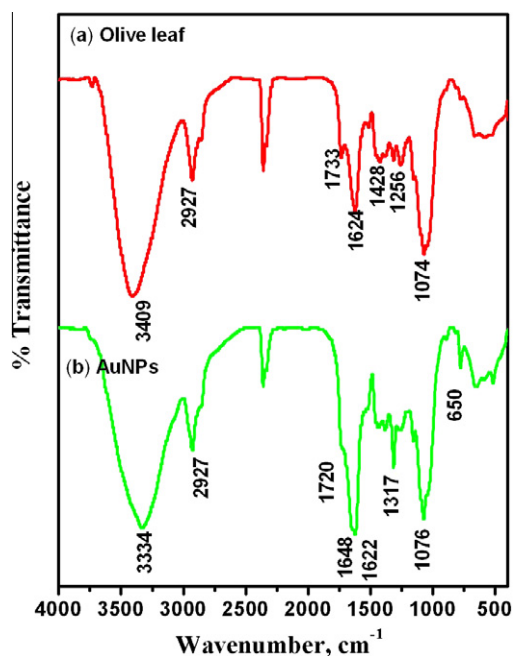
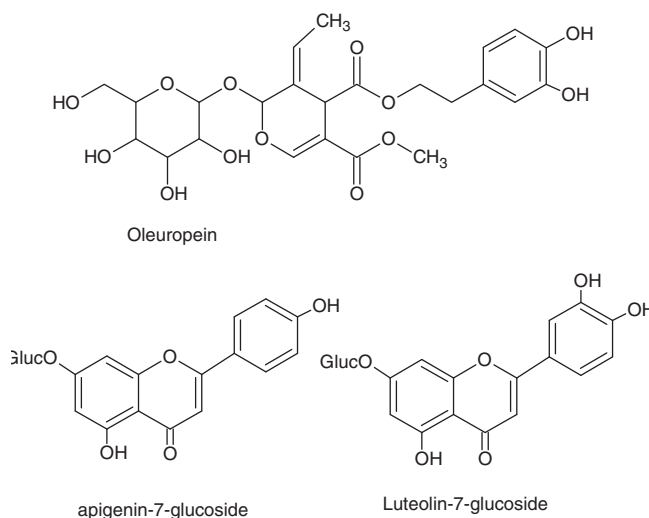


Figure 5 FTIR spectra of (a) a plain olive leaf and (b) capped AuNPs.



Scheme 1

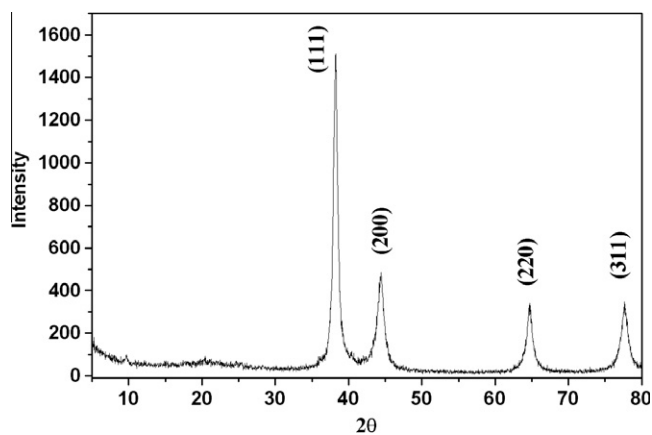


Figure 6 XRD pattern of dried powder of gold nanoparticles.

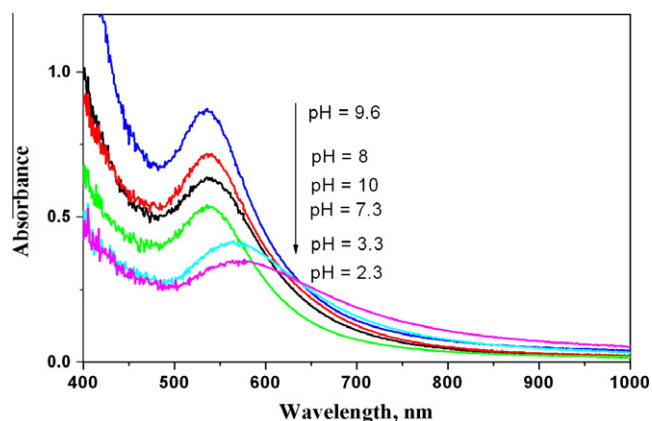


Figure 7 Effect of the pH on the SPR of AuNPs (2 ml extract, 1.3×10^{-4} M Au^{3+}).

capping of and efficient stabilization of the bio-reduced gold nanoparticles. Fig. 5 shows the FTIR spectra of the olive leaf extract and AuNPs. The FTIR spectra reveal the presence of different functional groups. The IR bands (Fig. 5a) observed at 3409 and 1733 cm^{-1} in dried olive leaf are characteristic of the O—H and C=O stretching modes for the OH and C=O groups possibly of oleuropein, apigenin-7-glucoside and/or luteolin-7-glucoside present in it, (Scheme 1). The very strong band at 1077 cm^{-1} could be assigned to the C—OH vibrations of the protein in the olive leaf. The IR spectrum of AuNPs exhibit a medium intense band at 1721 cm^{-1} assigned to the C=O stretching mode (Fig. 5b). The shift of C=O stretching frequency indicates a bounding of the biomol-

ecules to the Au nanoparticles through this group. The band at 1624 cm^{-1} in the olive leaf extract assigned as amide I vibrations has become more prominent in the spectrum of gold and split into two bands at 1622 and 1648 cm^{-1} . It is well-known that proteins can bind to Au nanoparticles through the free amine groups or carboxylate ions of the amino acid residues in it. The presence of the IR bands due to C=O stretching vibrations at 1721 cm^{-1} and the appearance of amide I bands with a shift from that of the plain leaf indicate the possibility that gold nanoparticles are bound to proteins and antioxidant molecules through free amine groups and C=O, OH groups, respectively.

3.4. XRD

X-ray diffraction was used to confirm the crystalline nature of the particles. Fig. 6 shows a representative XRD pattern of the gold nanoparticles synthesized by the olive leaf extract after the complete reduction of Au^{3+} to Au^0 . A number of Bragg reflections were present which can be indexed on the basis of the face centered cubic *fcc* structure of gold. The diffraction peaks at $2\theta = 38.31^\circ$ (1 1 1), 44.46° (2 0 0), 64.67° (2 2 0) and 77.45° (3 1 1) obtained are identical with those reported for the standard gold metal (Au^0) (Joint Committee on Powder Diffraction Standards-JCPDS, USA) Thus, the XRD pattern suggests that the gold nanoparticles were essentially crystalline.

The ratio between the intensity of (2 0 0) and (1 1 1) diffraction peaks of 0.32 is lower than the conventional bulk intensity ratio (0.52), suggesting that (1 1 1) plane is the predominant orientation as confirmed by high-resolution TEM measurements. Similar results were reported earlier for gold nanoparticles (Philip, 2009; Li et al., 2007; Jeong et al., 2009). The average crystallite size according to Scherrer equation calculated using the width of the (1 1 1) peak is found to be 13 nm and is in good agreement with the particle size obtained from the TEM image at 5 ml of extract concentration.

3.5. Effect of pH

Fig. 7 shows the effect of the pH on the formation of gold nanoparticles. It can be seen that the absorbance increases with increasing pH up to pH 9.6 with a blue shift in the spectra. The color changed from blue in acidic medium to red purple in basic medium. At acidic pH, the particles size is expected to be larger than at the basic pH, as a red shift was clearly reported in the SPR spectra (Haiss et al., 2007). This result was confirmed by TEM measurements at pH 3.3 and 9.6 (Fig. 8). The size of the particles at pH 3.3 was larger while forming

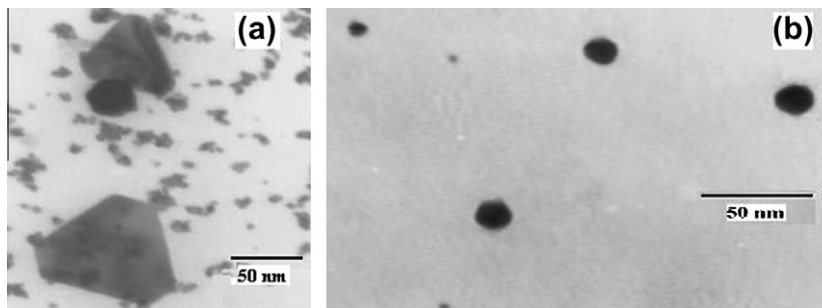


Figure 8 TEM images of AuNPs at (a) pH 3.3 and (b) pH 9.6.

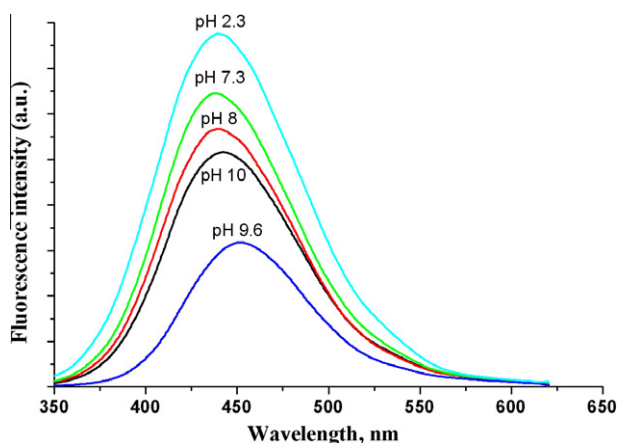


Figure 9 Photoluminescence of AuNPs as a function of pH ($\lambda_{\text{ex}} = 320 \text{ nm}$).

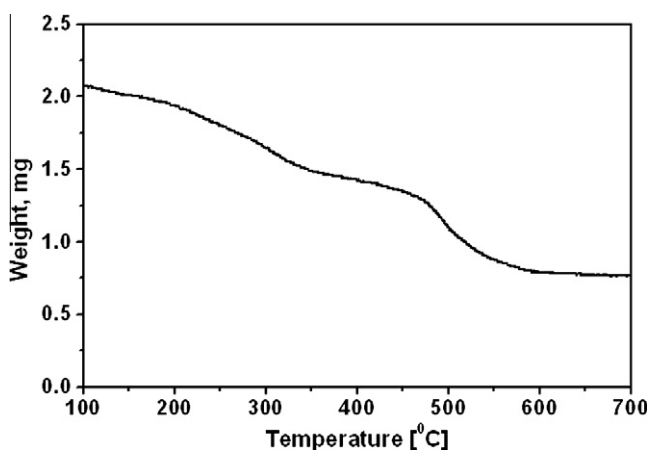


Figure 10 TGA of capped AuNPs prepared using an olive leaf extract.

hexagonal structures. Furthermore, the particles formed in acidic medium were unstable and precipitated within 12 h. The PL spectra of AuNPs as a function of pH are shown in Fig. 9. The fluorescence quenches as a function of increasing pH from 2.3 to 9.6 with a slight shift to longer wavelengths, and then increases again at pH 10. This behavior is in reverse to surface plasmon resonance shown in Fig. 7 and can be explained by the fact that an increasing of pH will make the capping of the nanoparticles' surface more efficient and supports the formation of smaller nanoparticles. This again suggests that the PL of the AuNPs depends on the nature and structure of the capping biomolecules.

3.6. Thermal study

The TGA plot of the capped gold nanoparticles prepared using high olive leaf extract (Fig. 10) showed a steady weight loss in the temperature range of 100–550 °C. The weight loss of the nano powder due to the desorption of bioorganic compounds in the AuNPs was 62.35%.

4. Conclusion

The high phenolic content of the hot water extract of olive leaves having strong anti-oxidant properties helped in the

reduction of gold cations to AuNPs. The characterization of AuNPs revealed that the morphology of the AuNPs depends on the extract concentration and pH of the used medium. At higher concentration of the extract and basic pH, the pseudo-spherical particles are capped by phytochemicals. This method for AuNP synthesis does not use any toxic reagent and thus has a great potential for the use in biomedical applications and will play an important role in future opto-electronic and biomedical device applications.

References

- Ankamwar, B., Chaudhary, M., Sastry, M., 2005. Gold nanotriangles biologically synthesized using tamarind leaf extract and potential application in vapor sensing. *Synth. React. Inorg. Met. Org. Nanomet. Chem.* 35, 19–26.
- Aslan, K., Perez-Luna, V.H., 2002. Surface modification of colloidal gold by chemisorption of alkanethiols in the presence of a nonionic surfactant. *Langmuir* 18, 6059–6065.
- Aziz, N.H., Farag, S.E., Mousa, L.A., Abo-Zaid, M.A., 1998. Comparative antibacterial and antifungal effects of some phenolic compounds. *Microbios* 93, 43–54.
- Benavente-García, O., Castillo, J., Lorente, J., Ortuño, A., Del Rio, J.A., 2000. Antioxidant activity of phenolics extracted from *Olea europaea* L. leaves. *Food Chem.* 68, 457–462.
- Bianco, A., Uccella, N., 2000. Biophenolic components of olives. *Food Res. Int.* 33, 475–485.
- Bisignano, G., Tomaino, A., Lo Cascio, R., Crisafi, G., Uccella, N., Saija, A., 1999. On the in vitro antimicrobial activity of oleuropein and hydroxytyrosol. *J. Pharm. Pharmacol.* 51, 971–974.
- Caruso, D., Berra, B., Giavarini, F., Cortesi, N., Fedeli, E., Galli, G., 1999. Effect of virgin olive oil phenolic compounds on in vitro oxidation of human low density lipoproteins. *Nutr. Metab. Cardiovasc. Dis.* 9, 102–107.
- Chandran, S.P., Chaudhary, M., Pasricha, R., Ahmad, A., Sastry, M., 2006. Synthesis of gold nanotriangles and silver nanoparticles using *Aloe vera* plant extract. *Biotechnol. Progr.* 22, 577–583.
- Daniel, M.-C., Astruc, D., 2004. Gold nanoparticles: assembly, supramolecular chemistry, quantum-size-related properties, and applications toward biology, catalysis, and nanotechnology. *Chem. Rev.* 104, 293.
- Das, R.K., Borthakur, B.B., Bora, U., 2010. Green synthesis of gold nanoparticles using ethanolic leaf extract of *Centella asiatica*. *Mater. Lett.* 64, 1445–1447.
- de la Puerta, R., Martínez-Domínguez, E., Ruiz-Gutiérrez, V., 2000. Effect of minor components of virgin olive oil on topical anti-inflammatory assays. *Z. Naturforsch. [C]* 55, 814–819.
- Dubeya, S.P., Lahtinen, M., Sillanpää, M., 2010. Tansy fruit mediated greener synthesis of silver and gold nanoparticles. *Process Biochem.* 45, 1065–1071.
- Farag, R.S., El-Baroty, G.S., Basuny, A.M., 2003. Safety evaluation of olive phenolic compounds as natural antioxidants. *Int. J. Food Sci. Nutr.* 54, 159–174.
- Furneri, P.M., Marino, A., Saija, A., Uccella, N., Bisignano, G., 2002. In vitro antimycoplasmal activity of oleuropein. *Int. J. Antimicrob. Agents* 20, 293–296.
- Ghodake, G.S., Deshpande, N.G., Lee, Y.P., Jin, E.S., 2010. Pear fruit extract-assisted room-temperature biosynthesis of gold nanoplates. *Colloids Surf. B: Biointerfaces* 75, 584–589.
- Haick, H., 2007. Chemical sensors based on molecularly modified metallic nanoparticles. *J. Phys. D: Appl. Phys.* 40, 7173–7186.
- Haiss, W., Thanh, N.T.K., Aveyard, J., Fernig, D.G., 2007. Determination of size and concentration of gold nanoparticles from UV–Vis spectra. *Anal. Chem.* 79, 4215–4221.
- Hanbury, D., 1854. On the febrifuge properties of the olive (*Olea europaea*, L.). *Pharmaceut. J. Provincial Trans.*, 353–354.

- He, S., Zhang, Y., Guo, Z., Gu, N., 2008. Biological synthesis of gold nanowires using extract of *Rhodospseudomonas capsulata*. *Biotechnol. Progr.* 24, 476–480.
- Hostetler, M.J., Wingate, E., Zhong, C.J., Harris, E., Vachet, W., Clark, M.R., Londono, J.D., Green, S.J., Stokes, J.J., Wignall, D., Glish, L., Porter, M.D., Evans, N.D., Murray, W., 1998. Alkanethiolate gold cluster molecules with core diameters from 1.5 to 5.2 nm: core and monolayer properties as a function of core size. *Langmuir* 14, 17–30.
- Huang, S.H., 2006. Gold nanoparticle-based immunochromatographic test for identification of *Staphylococcus aureus* from clinical specimens. *Clin. Chim. Acta* 373, 139.
- Husseiny, M.I., El-Aziz, M.A., Badr, Y., Mahmoud, M.A., 2007. Biosynthesis of gold nanoparticles using *Pseudomonas aeruginosa*. *Spectrochim. Acta A* 67, 1003.
- Jeong, G.W., Lee, Y.W., Kim, M., Han, S.W., 2009. High-yield synthesis of multi-branched gold nanoparticles and their surface-enhanced Raman scattering properties. *J. Colloid Interface Sci.* 329, 97–102.
- Juven, B., Henis, Y., 1970. Studies on the antimicrobial activity of olive phenolic compounds. *J. Appl. Bacteriol.* 33, 721–732.
- Kalishwaralal, K., Deepak, V., Ram Kumar Pandian, S., Kottaisamy, M., Barathmani, K.S., Kartikeyan, B., Gurunathan, S., 2010. Biosynthesis of silver and gold nanoparticles using *Brevibacterium casei*. *Colloids Surf. B: Biointerfaces* 77, 257–262.
- Kato, N., Caruso, F., 2005. Homogeneous, competitive fluorescence quenching immunoassay based on gold nanoparticle/polyelectrolyte coated latex particles. *J. Phys. Chem. B* 109, 19604.
- Krpeti, Z., Scar, G., Caneva, E., Speranza, G., Porta, F., 2009. Gold nanoparticles prepared using cape aloe active components. *Langmuir* 25, 7217–7221.
- Kumar, V., Yadav, S.K., 2008. Plant-mediated synthesis of silver and gold nanoparticles and their applications. *J. Chem. Technol. Biotechnol.* 84, 151–157.
- Lee, O.H., Lee, B.Y., Lee, J., Lee, H.B., Son, J.Y., Park, C.S., Shetty, K., Kim, Y.C., 2009. Assessment of phenolics-enriched extract and fractions of olive leaves and their antioxidant activities. *Bioresour. Technol.* 100, 6107–6113.
- Lee-Huang, S., Zhang, L., Huang, P.L., Chang, Y.-T., Huang, P.L., 2003. Anti-HIV activity of olive leaf extract (OLE) and modulation of host cell gene expression by HIV-1 infection and OLE treatment. *Biochem. Biophys. Res. Commun.* 307, 1029–1037.
- Lengke, M.F., Fleet, M.E., Southan, G., 2006. Morphology of gold nanoparticles synthesized by filamentous Cyanobacteria from gold(I)-thiosulfate and gold(III)-chloride complexes. *Langmuir* 22, 2780.
- Li, S., Shen, Y., Xie, A., Yu, X., Zhang, X., Yang, L., Li, C., 2007. Rapid, room-temperature synthesis of amorphous selenium/protein composites using *Capsicum annuum* L. extract. *Nanotechnology* 18, 405101.
- Link, S., El-Sayed, M.A., 2000. Shape and size dependence of radiative, non-radiative and photothermal properties of gold nanoparticles. *Int. Rev. Phys. Chem.* 19, 409.
- Mata, Y.N., Torres, E., Blázquez, M.L., Ballester, A., González, F., Muñoz, J.A., 2009. Gold (III) biosorption and bioreduction with the brown alga *Fucus vesiculosus*. *J. Hazard. Mater.* 166, 612–618.
- Mishra, A.N., Bhadauria, S., Gaur, M.S., Pasricha, R., Kushwah, B.S., 2010. Synthesis of gold nanoparticles by leaves of zero-calorie sweetener herb (*Stevia rebaudiana*) and their nanoscopic characterization by spectroscopy and microscopy. *Int. J. Green Nanotechnol.: Phys. Chem.* 1 (2), 118–124.
- Mulvaney, P., 1996. Surface plasmon spectroscopy of nanosized metal particles. *Langmuir* 12, 788–800.
- Philip, D., 2009. Biosynthesis of Au, Ag and Au–Ag nanoparticles using edible mushroom extract. *Spectrochim. Acta, Part A* 73, 374–381.
- Philip, D., 2010. Green synthesis of gold and silver nanoparticles using *Hibiscus Rosa sinensis*. *Physica E* 42, 1417–1424.
- Rajasekharreddy, P., Rani, P.U., Sreedhar, B., 2010. Qualitative assessment of silver and gold nanoparticle synthesis in various plants: a photobiological approach. *J. Nanopart. Res.* 12, 1711–1721.
- Raveendran, P., Fu, J., Wallen, S.L., 2003. Completely green synthesis and stabilization of metal nanoparticles. *J. Am. Chem. Soc.* 125, 13940–13941.
- Schmidt, K., von Banchet, G.S., Heppelmann, B., 1999. *J. Neurosci. Methods* 87, 195–200.
- Shankar, S.S., Ahmad, A., Parsricha, R., Sastry, M., 2003. Bioreduction of chloroaurate ions by geranium leaves and its endophytic fungus yields gold nanoparticles of different shapes. *J. Mater. Chem.* 13, 1822.
- Shankar, S.S., Rai, A., Ahmad, A., Sastry, M., 2004. Rapid synthesis of Au, Ag, and bimetallic Au core Ag shell nanoparticles using *Neem (Azadirachta indica)* leaf broth. *J. Colloid Interface Sci.* 275, 496–502.
- Smitha, S.L., Nissamudeen, K.M., Philip, D., Gopchandran, K.G., 2008. Studies on surface plasmon resonance and photoluminescence of silver nanoparticles. *Spectrochim. Acta A* 71, 186.
- Smitha, S.L., Philip, D., Gopchandran, K.G., 2009. Green synthesis of gold nanoparticles using *Cinnamomum zeylanicum* leaf broth. *Spectrochim. Acta A* 74, 735–739.
- Song, J.Y., Jang, H.-K., Kim, B.S., 2009. Biological synthesis of gold nanoparticles using *Magnolia kobus* and *Diopyros kaki* leaf extracts. *Process Biochem.* 44, 1133–1138.
- Sosa, I.O., Noguez, C., Barrera, R.G., 2003. Optical properties of metal nanoparticles with arbitrary shapes. *J. Phys. Chem. B* 107, 6269–6275.
- Sperling, R.A., Gil, P.R., Zhang, F., Zanella, M., Parak, W.J., 2008. Biological applications of gold nanoparticles. *Chem. Soc. Rev.* 37, 1896–1908.
- Thakkar, K.N., Mhatre, S.S., Parikh, R.Y., 2010. Biological synthesis of metallic nanoparticles. *Nanomed. Nanotechnol. Biomed.* 6, 257–262.
- Visioli, F., Bellosta, S., Galli, C., 1998. Oleuropein, the bitter principle of olives, enhances nitric oxide production by mouse macrophages. *Life Sci.* 62, 541–546.
- Wilson, R., 2008. The use of gold nanoparticles in diagnostics and detection. *Chem. Soc. Rev.* 37, 2028–2045.
- Xie, J.P., Lee, J.Y., Wang, D.L.C., Ting, T.P., 2007. Identification of active biomolecules in the high yield synthesis of single-crystalline gold nanoplates in the alga solutions. *Small* 4, 672–682.
- Xu, J., Craig, S.L., 2005. Thermodynamics of DNA hybridization on gold nanoparticles. *J. Am. Chem. Soc.* 127, 13227–13231.
- Ziogas, V., Tanou, G., Molassiotis, A., Diamantidis, G., Vasilakakis, M., 2010. Antioxidant and free radical-scavenging activities of phenolic extracts of olive fruits. *Food Chem.* 120, 1097–1103.